Materials Physics and Mechanics 32 (2017) 43-50 Received: May 29, 2017

SCALING OF LOW FIELD MAGNETOELASTIC HYSTERESIS IN ANTIFERROMAGNETIC DY

Iu. Liubimova[1*], M. L. Corró[2], J. Torrens-Serra[2], V. Recarte[3], J.-I. Pérez-Landazábal[3], S. Kustov[1,2]

[1] ITMO University, 49 Kronverkskiy av., St Petersburg 197101, Russia

[2] Department of Physics, University of Balearic Islands, Cra. Valldemossa km 7.5, Palma de Mallorca E07122, Spain

[3] Universidad Pública de Navarra (UPNA), Campus Arrosadia, 31006 Pamplona, Spain

*e-mail: liubimovaiuliia@corp.ifmo.ru

Abstract. We investigate reversible inverse magnetostriction in order to study scaling properties of magnetic hysteresis in the helical antiferromagnetic phase of polycrystalline Dy. We argue that the experimental method used is more sensitive than studies of conventional magnetic hysteresis. This advantage allows us to study hysteretic properties of antiferromagnetic Dy over the temperature ranges, not accessible previously. We introduce generalized coercivity of magnetoelastic hysteresis and show that it demonstrates, under different experimental protocols, the same exponents of scaling power laws in the ferro- and antiferromagnetic phases. The similarity of hindering mechanisms impeding the mobility of domain walls in antiferromagnetic and ferromagnetic phases is suggested as the reason of the observed universality of hysteresis scaling.

1. Introduction

Magnetization of ferromagnets due to domain wall (DW) motion occurs, under slowly increasing field, through their cooperative avalanche-like displacements, manifested as Barkhausen jumps. Cooperative dynamics of defects in many systems belong to a few universality classes [1] with power-law distributed avalanche sizes and durations [1, 2]. Studies of scaling power laws in magnetic hysteresis are quite deep, see e.g. [2–5]. Much less is known, in terms of scaling, on DW dynamics in antiferromagnets, due to the absence of macroscopic magnetization associated with DW motion. Kobayashi [3] has recently studied scaling of conventional *B(H)* hysteresis loops in polycrystalline Dy at low fields up to 20 kA/m. Experiments were performed both in ferro- and helical antiferromagnetic phases. Hysteresis losses, ΔW_{loss}, plotted against remanent flux density, B_r, yielded power law dependences $\Delta W_{loss} \propto (B_r)^n$ with the same exponents n = 1.5 for the antiferromagnetic (AFM) and ferromagnetic (FM) phases [3]. The universality of scaling of $\Delta W_{loss}(B_r)$ in the FM and AFM phases was attributed to the similarity of dissipative properties of DW motion. The hysteresis in Ref. 3 was studied only on heating from the FM phase and only up to 130 K. The sensitivity of the experimental equipment was not sufficient to study magnetic hysteresis in the AFM phase on cooling and on heating from the FM phase above 130 K. A strong difference is usually observed between magnetic, elastic and other properties of Dy, other rare earth metals and their alloys, measured in the AFM phase on cooling and on heating from the FM phase. This

difference is referred to as thermal hysteresis. The origin of thermal hysteresis has been studied for decades using a variety of experimental techniques [6–10]. The common interpretation of thermal hysteresis suggests that type I domain walls are inherited by AFM phase from ferromagnetic DWs of the FM phase. Type I DWs in helical AFM structures are perpendicular to the c-axis of the hexagonal lattice, separate spin chains with opposite rotation directions and possess net magnetic moment. The reason for their disappearance (and, hence, the disappearance of the thermal hysteresis) at a certain temperature and the value of this temperature remained an open issue.

It has recently been shown that the thermal hysteresis in polycrystalline Dy is limited by the temperature of the Villari point T_{VP} = 166 K, in which the magnetostriction changes the sign [11]. Detailed studies of the reversible Villari effect (RVE) have shown that the thermal hysteresis is indeed related to residual FM phase, but different from the type I DWs. Lattice defects, creating high elastic strain, like dislocations, were suggested as species that locally stabilize the residual FM phase. Since lattice strains are involved in stabilization of residual FM phase, the stabilization operates only up to the Villari point, in which the sign of magnetoelastic coupling changes. Suggested mechanisms of thermal hysteresis imply that the study of scaling performed by Kobayashi [3] dealt with the AFM phase containing certain elements possessing net moments, inherited from the FM phase. The data for "pure" AFM phase with very narrow magnetic hysteresis could not be obtained experimentally.

We suggest using RVE versus H hysteresis (which can be referred to as magnetoelastic hysteresis) instead of conventional $B(H)$ loops to investigate scaling of hysteresis in AFM Dy. The width of the RVE loop corresponds to the condition $M = 0$ instead of $B = 0$, valid for conventional $B(H)$ hysteresis. Therefore, the width and the area of RVE versus H loops can rather easily be detected in the AFM phase, when magnetic susceptibility, $\chi << 1$ [12]. This advantageous property of RVE hysteresis enables us to study scaling properties both on heating from the FM state over the entire temperature range of existence of helical AFM phase, and on cooling, in the "pure" AFM phase. The present work reports the results of such experiments in polycrystalline Dy at low periodic applied fields.

2. Material and experimental technique

Dysprosium is a rare earth element with a paramagnetic (PM) - helical-type antiferromagnetic transition at a Néel temperature, T_N =178 K. During FM ordering at lower temperatures, the hexagonal lattice of antiferromagnetic Dy undergoes orthorhombic distortions. Therefore, the AFM-FM transition becomes a first order magnetostructural transition with the Curie temperature on cooling, T_C ~ 85 K [13–17]. Samples used in the present study (1.0× 1.3× 12.2 mm^3) were spark cut from a sheet of polycrystalline dysprosium of 99.9 wt% purity, supplied by Sigma Aldrich.

A method referred to as mechanomagnetic spectroscopy [18–20] was used to register the reversible Villari effect, or reversible inverse magnetostriction. The experimental technique employs resonant Piezoelectric Ultrasonic Composite Oscillator Technique (operating at a frequency around 90 kHz) [21, 22] with an additional channel for magnetic measurements. A longitudinal standing wave in the fundamental mode is excited in a sample. The flux density induced by oscillatory stress in the strain antinode is detected using a small pickup coil, located around middle section of the sample. The received signal is decomposed then into the real and imaginary components (with respect to stress/strain) by means of a lock-in amplifier. Since the real part of strain/stress-induced flux density is much higher than the imaginary one, only the former will be analyzed hereafter.

The experimental setup operates at oscillatory strain amplitudes ε_0 from 10^{-7} to 10^{-4}, temperatures T between 80 and 400 K and under axial magnetic fields H up to 18 kA/m. A detailed description of the method and experimental setup can be found elsewhere [19–22]. In

the present work the amplitude of the real part of periodic stress/strain-induced flux density, B_0, will be reported. B_0 was registered as a function of the periodic magnetic field with variable amplitude H_0 at different selected temperatures and at a fixed elastic strain amplitude $\varepsilon_0 = 10^{-5}$. The $B_0(H)$ dependences were measured during interruptions of cooling or heating of the sample over the temperature ranges: a) between 250 and 95 K (only paramagnetic – antiferromagnetic transition); b) 250-80 K (temperature range covering the transition to the ferromagnetic phase). The amplitude H_0 of the saw-tooth magnetic field with a frequency of 0.001 Hz varied between 0.28 kA/m and 18 kA/m. Each $B_0(H)$ loop contained 150 experimental points. The measurement of a set of $B_0(H)$ loops with different field amplitudes H_0 will be referred to as a field scan (or H_0 scan).

3. Results and discussion

Figure 1 shows the results of field scans for several selected temperatures, performed under different protocols: cooling the sample (a), heating the sample from 95 K (i.e. during thermal cycling within AFM phase), (b), and heating from 80 K (from the FM phase), (c). Data in Fig. 1 (a), (b), (c) correspond to the AFM phase. Panel (d) shows similar $B_0(H)$ loops in the FM phase, at the lowest temperature of the thermal cycle, T = 80 K. Fig. 1(e) displays $B_0(H)$ hysteresis in the vicinity of the Villari point. The data shown in Fig. 1 correspond to increasing H_0. Each field scan was performed for the thermally demagnetized state of the sample. Before each H_0 scan the sample was held for 20 min at a constant temperature in order to minimize time dependence of the B_0 signal due to the RVE relaxation observed on heating from the FM phase [11].

A crucial effect in the data of Fig. 1 is the change of the slope of the hysteresis loops (HL) between 140 and 173 K. This qualitative change occurs upon crossing the Villari point reported previously at T_{VP} =166 K [11]. Apart from magnetostriction, the Villari point marks qualitative changes in the behavior of such canonical property as magnetic susceptibility [12]. If thermal cycling is restricted to the AFM phase, HLs are essentially the same for corresponding temperatures during cooling and heating, cf. columns (a) and (b) in Fig. 1. The results obtained during heating from the FM phase are qualitatively different, (c). The most prominent features provoked by the excursion to the FM phase are:

- a dramatic increase of the HL width, as compared to the thermal cycles in the helical AFM phase. This difference disappears at the T_{VP} = 166 K [11], in between the temperatures of 140 and 173 K, cf. columns (c) and (a), (b);
- a recovery of the same shape of HLs in the helical AFM phase in all three experiments between the T_{VP} = 166 K and T_N [11], cf. the HLs at 173 K in Fig. 1.

$B_0(H)$ HLs have already been qualitatively described and analyzed quantitatively for a fixed value of H_0 [11, 12]. In the present work we employ field scans and quantify the HL area in H_0 scans. The HL area, ΔA, was determined by numerical integration using standard procedure:

$$\Delta A = \oint B_0 dH . \tag{1}$$

Apart from the HL area, we suggest to consider an additional parameter, which can be classified as effective hysteresis H^*. Equation (1) can be rewritten:

$$\Delta A = \oint B_0 dH = 4B_0^{\max} H^*, \tag{2}$$

where B_0^{max} is the maximum B_0 value in a field cycle and H^* – average semiwidth of the $B_0(H)$ hysteresis loop, or effective hysteresis.

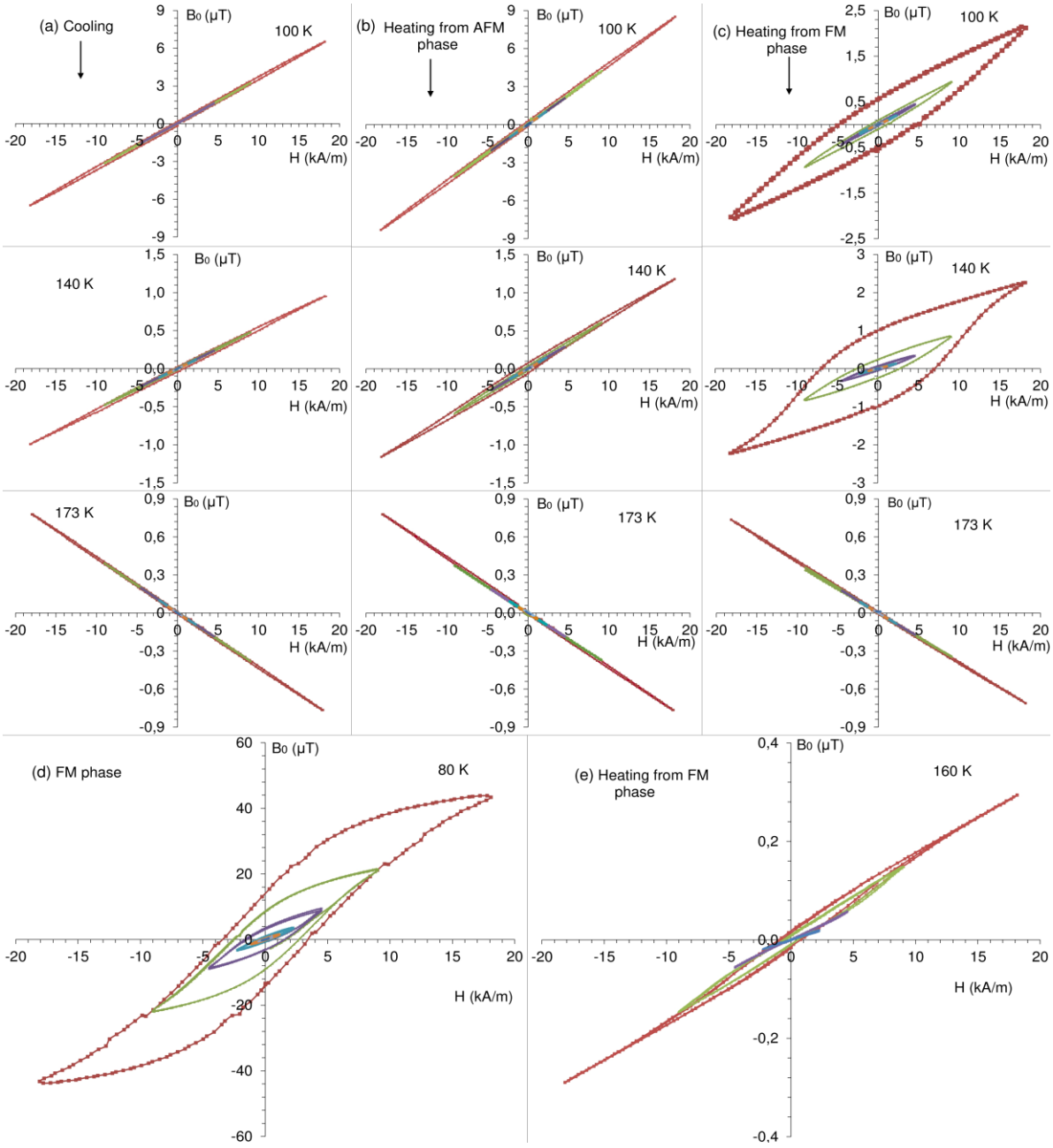

Fig. 1. Real part of the amplitude of the stress-induced flux density, B_0, versus periodic field with increasing amplitude H_0: 0.28, 0.56, 1.13, 2.25, 4.5, 9, 18 kA/m at several selected temperatures T = 100, 140 and 173 K:
(a) cooling;
(b) heating from 95 K (thermal cycling within the antiferromagnetic phase);
(c) heating from 80 K (from the ferromagnetic phase).
Panels (d) and (e) show $B_0(H)$ loops registered at 80 K in the FM phase and at 160 K (in the antiferromagnetic phase) during heating from 80 K.
Frequency of applied magnetic field 0.001 Hz, oscillatory strain amplitude $\varepsilon_0 = 10^{-5}$.

Similar parameter is introduced in conventional *B(H)* hysteresis [23] and is considered as generalized coercivity, which takes into account all processes occurring along the hysteresis loop, like DW nucleation, motion, magnetization rotation, etc. In the present case, these different processes include the properties associated both with AFM and residual FM phases, at least for heating scans from 80 K. From Eq. (2) one easily gets

$$H^* = \frac{\Delta A}{4B_0^{\max}}. \qquad (3)$$

Equation (3) is similar to the definition of generalized *B(H)* hysteresis [23] in which $B_0^{\max}$ substitutes for the maximum magnetization value. It is worth to emphasize that, although the area of the magnetoelastic loop $B_0(H)$ does not represent dissipated energy, the effective hysteresis H^* defined from Eq. (3) has a clear physical sense, since the coercivity of the $B_0(H)$ loop is the coercivity of *M(H)* hysteresis [12].

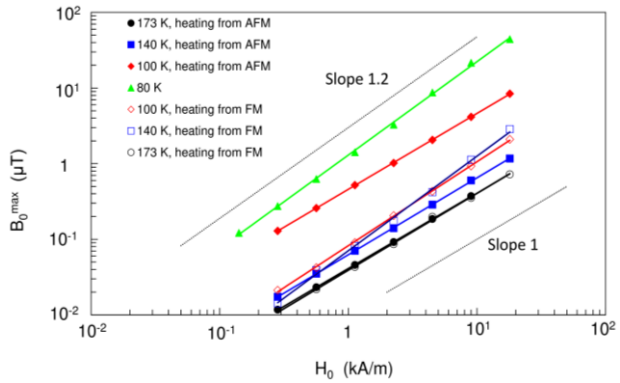

Fig. 2. Amplitude of the stress-induced flux density, $B_0^{\max}$, as a function of the amplitude of cyclic magnetic field, H_0, for several selected temperatures, 100, 140, 173 K on heating from 80 K (from the ferromagnetic phase) and heating from 95 K (thermal cycle within AFM phase). The data taken in the ferromagnetic phase at 80 K are also shown. Oscillatory strain amplitude $\varepsilon_0 = 10^{-5}$, frequency of applied magnetic field 0.001 Hz.

Figure 2 is the synthetic plot of $B_0^{\max}$ versus H_0 at different temperatures and thermal cycling protocols. All dependences are well fitted with a power law

$$B_0^{\max} \propto (H_0)^m. \qquad (4)$$

For thermal cycles within AFM phase, the exponent m = 1. B_0 is the reversible inverse magnetostriction, which can be approximately taken as differential inverse magnetostriction if the narrow hysteresis in the "pure" AFM phase is disregarded. Then the linear $B_0^{\max}(H_0)$ dependence simply reflects the parabolic field dependence of magnetostriction in the AFM phase [24]. Quite remarkable is that the exponent m takes different values close to 1.2 both in the FM phase at 80 K and during heating from this temperature (see the dependences registered at 100 and 140 K in Fig. 2), despite significant difference in the absolute values of B_0 at 80 K and at 140 K. Thus, according to Fig. 2, the exponent m in Eq. (4) is the same for the FM phase and for the AFM phase in heating scans from 80 K, but differs for the AFM phase on heating from 95 K (and also on cooling, not shown in Fig. 2). This result is consistent with the hypothesis that thermal hysteresis is due to residual FM phase. Above the Villari point, as is expected from the HLs in Fig. 1, all $B_0^{\max}(H_0)$ dependences collapse into the same trend.

Figure 3 shows $\Delta A(B_0^{\max})$ dependences derived from H_0 scans at selected temperatures under different thermal cycling protocols. Figure 3(a) displays the $\Delta A(B_0^{\max})$ dependences for cooling and for heating from 80 K (from the FM phase). Similar data for heating scans from 95 and 80 K (from the AFM and FM phases, respectively) are compared in Fig. 3(b). Fig. 3(b) depicts also the $\Delta A(B_0^{\max})$ dependences for 80 K, the lowest temperature of thermal cycles, and 160 K, the temperature close to the Villari point at 166 K (see the inset).

All dependences fit the same power law in which the variables are separated:

$$\Delta A(B_0^{\max}, T) = \Delta A_n(T)\left(\frac{B_0^{\max}}{B_n}\right)^{\alpha}, \quad (5)$$

where B_n is a constant which we take B_n = 1 T, and $A_n(T)$ is a function of only temperature. The average value of the exponent α is 2.2 ± 0.12 for all dependences on cooling and heating from both phases. The similarity of the slopes of $\Delta A(B_0^{\max})$ dependences is observed, despite a significant difference, of the order of 10^2-10^3 of the ΔA magnitudes. From Eqs. (3) and (5) one immediately gets that the generalized hysteresis $H^*(B_0^{\max})$ is also a power law with the same exponent $\beta = \alpha - 1$ in the AFM and FM phases and under different thermal cycling protocols:

$$H^* \propto \left(B_0^{\max}\right)^{\beta}. \quad (6)$$

The results depicted in Fig. 3 deserve further minor comments.

- The separation of variables and scaling, Eq. (5), break down in a narrow temperature range close to the T_{VP} if the sample is heated from the FM phase. In that case the HLs deviate strongly from nearly linear shape, see Fig. 1(e). The inset in Fig. 3(b) exemplifies this deviation from a power law for a scan at 160 K.

- The maximum value of the RVE in a cycle of applied magnetic field, $B_0^{\max}$, is used as the argument for the data in Fig. 3. Therefore, a dramatic decrease of the RVE for the temperatures close to the T_{VP} is revealed in the data of Fig. 3 as a shift of the curves at 173 K and especially at 160 K (the inset) along the x-axis.

The present results reveal power law dependences of the area of magnetoelastic hysteresis $\Delta A\left(B_0^{\max}\right)$ and of the generalized coercivity $H^*(B_0^{\max})$ with the same universal exponent in the FM and AFM phases, as well as on cooling and heating from AFM and FM phases. This result seems to support the conclusion drawn by Kobayashi [3] about similarity of dissipation mechanisms involved in the helical AFM and FM phases of Dy. The data obtained previously [3] for the AFM phase referred, likely, to the mixture of "pure" AFM and residual FM phases. The present results extend the conclusion on the similarity of the hindrance mechanism of DW motion to the AFM phase, which persists on cooling and, supposedly, does not contain residual FM inclusions. The exponent in $H^*(B_0^{\max})$ power law derived from magnetoelastic hysteresis is $\beta = \alpha - 1 = 1.2$. This value is different from the exponent (0.6-0.7) typical for the empirical Steinmetz law [3–5, 25]. This discrepancy is expected, since the magnetoelastic hysteresis $B_0(H)$ reported in the present study is different from the conventional magnetic hysteresis $B(H)$. One of the feasible origins of the universal hindrance mechanism for DW motion is interaction with lattice dislocations. According to Ref. 12, for the samples heated from the FM phase, the imaginary component of susceptibility shows a sharp decline at the temperature of Villari point, where dislocations are expected to loose local residual ferromagnetic ordering. This fact served as the indication that lattice dislocations control dissipation during of DW motion [12]. The results of the present work extend this conclusion to both FM and AFM phases under different experimental protocols.

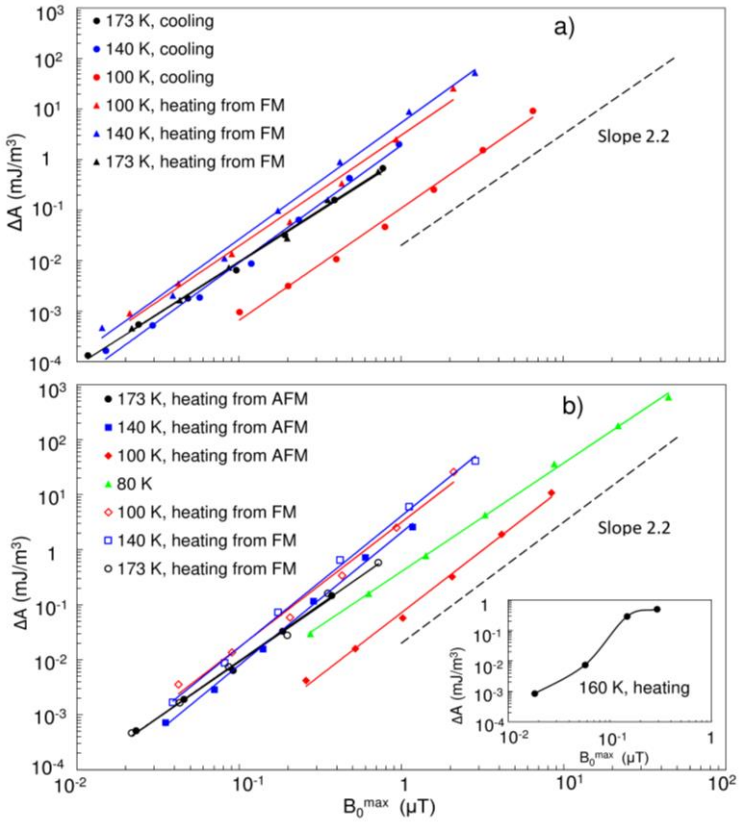

Fig. 3. Area of the $B_0(H)$ hysteresis loop, ΔA, as a function of amplitude of the stress-induced flux density, B_0^{max}, for several selected temperatures, 100, 140, 173 K:
(a) cooling and subsequent heating from 80 K (ferromagnetic phase);
(b) heating from 80 and from 95 K (from the ferromagnetic and antiferromagnetic phases, respectively).
Data registered in the ferromagnetic phase at 80 K are shown in (b) as well. The inset shows $\Delta A\left(B_0^{max}\right)$ dependence at 160 K (close to Villari point at 166 K) registered for increasing temperatures from 80 K. Oscillatory strain amplitude $\varepsilon_0 = 10^{-5}$, frequency of periodic field 0.001 Hz.

4. Conclusion

Mechanomagnetic spectroscopy is an efficient method for studying narrow magnetic hysteresis in the AFM phases.

In the helical antiferromagnetic phase polycrystalline Dy, distinct dependences of the reversible Villari effect on periodic field amplitude, measured for increasing temperatures from the ferromagnetic state and during thermal cycling within the helical phase, are consistent with the hypothesis that the helical phase inherits local ferromagnetic order from the ferromagnetic state.

Scaling behavior of magnetoelastic hysteresis and of generalized coercivity is similar for the ferromagnetic and helical ferromagnetic phase of Dy. This observation is attributed to the similarity of the hindrance mechanism of domain wall motion.

Acknowledgements

This work was supported by the Ministry of Education and Science of Russian Federation, goszadanie 3.1421.2017/4.6 and the Spanish Ministerio de Economía y Competitividad, project

MAT2014-56116-C04-01-R and by the Government of the Russian Federation (Grant 074-U01) through the ITMO Fellowship and Professorship Program.

References

[1] E.K.H. Salje, K. Dahmen // *Annu. Rev. Condens. Matter Phys.* **5** (2014) 233.
[2] J.P. Sethna, K.A. Dahmen, C.R. Myers // *Nature* **410** (2001) 242.
[3] S. Kobayashi // *Phys. Rev. Lett.* **106** (2011) 057207.
[4] C.P. Steinmetz // *Proceedings of the IEEE* **72** (1984) 2.
[5] S. Kobayashi, S. Takahashi, T. Shishido, Ya. Kamada, H. Kikuchi // *J. Appl. Phys.* **107** (2010) 023908.
[6] A. Del Moral, E.W. Lee // *J. Phys. F: Metal Phys.* **4** (1974) 280.
[7] D.R. Behrendt, S. Legvold, F.H. Spedding // *Phys.Rev.* **109** (1958) 1544.
[8] T.J. McKenna, S.J. Campbell, D.H. Chaplin, G.V.H. Wilson // *Phys. Stat. Sol. (a)* **75** (1983) 421.
[9] T.J. McKenna, S.J. Campbell, D.H. Chaplin, G.V.H. Wilson // *J. Magn. Magn. Mater.* **20** (1980) 207.
[10] A.S. Chernyshov, Ya. Mudryk, V.K. Pecharsky, K.A. Gschneidner, Jr. // *Phys. Rev. B* **77** (2008) 094132.
[11] M.L. Corró, A. El Hichou, E. Cesari, and S. Kustov // *J. Phys. D: Appl. Phys.* **49** (2016) 015001.
[12] Iu. Liubimova, M.-L. Corró Moyà, J. Torrens-Serra, V. Recarte, J.I. Pérez-Landazábal, S. Kustov // *Metals* **7** (2017) 215.
[13] J. Elliott, S. Legvold, F. Spedding // *Phys. Rev.* **94** (1954) 1143.
[14] M. Griffel, R.E. Skochdopole, F.H. Spedding // *J. Chem. Phys.* **25** (1956) 75.
[15] M.K. Wilkinson, W.C. Koehler, E.O. Wollan, J.W. Cable // *J. Appl. Phys.* **32** (1961) 48S.
[16] F.J. Darnell // *Phys. Rev.* **130 (5)** (1963) 1825.
[17] F.J. Darnell, E.P. Moore // *J. Appl. Phys.* **34** (1963) 1337.
[18] D.C. Jiles // *J. Phys. D: Appl. Phys.* **28** (1995) 1537.
[19] S. Kustov, M.L. Corró, E. Cesari // *Mater. Sci. Eng. A* **521–522** (2009) 194.
[20] S. Kustov, F. Masdeu, E. Cesari // *Appl. Phys. Lett.* **89** (2006) 061917.
[21] S. Kustov, S. Golyandin, A. Ichino, G. Gremaud // *Mater. Sci. Eng. A* **442** (2006) 532.
[22] W.H. Robinson, A. Edgar // *IEEE Trans., Sonics and Ultrasonics* **21** (1974) 98.
[23] G. Bertotti, *Hysteresis in Magnetism* (Academic Press, San Diego, 1998) Chap. 10, p.297.
[24] M.L. Corró, A. El Hichou, S. Kustov // *J. Magn. Magn. Mater.* **400** (2016) 141.
[25] G. Bertotti, *Hysteresis in Magnetism* (Academic Press, San Diego, 1998) Chap. 9, p.255.